metabolites

MDPI

Article

Seasonal Variations and Interspecific Differences in Metabolomes of Freshwater Fish Tissues: Quantitative Metabolomic Profiles of Lenses and Gills

Yuri P. Tsentalovich [1,2,*], Vadim V. Yanshole [1,2], Lyudmila V. Yanshole [1,2], Ekaterina A. Zelentsova [1,2], Arsenty D. Melnikov [1,2] and Renad Z. Sagdeev [1,2]

1 International Tomography Center SB RAS, Institutskaya 3a, Novosibirsk 630090, Russia; vadim.yanshole@tomo.nsc.ru (V.V.Y.); lucy@tomo.nsc.ru (L.V.Y.); zelentsova@tomo.nsc.ru (E.A.Z.); melnikov.arsenty@tomo.nsc.ru (A.D.M.); rsagdeev@tomo.nsc.ru (R.Z.S.)

2 Novosibirsk State University, Pirogova 2, Novosibirsk 630090, Russia

* Correspondence: yura@tomo.nsc.ru; Tel.: +7-383-330-31-36; Fax: +7-383-333-13-99

Received: 16 October 2019; Accepted: 31 October 2019; Published: 2 November 2019

Abstract: This work represents the first comprehensive report on quantitative metabolomic composition of tissues of pike-perch (*Sander lucioperca*) and Siberian roach (*Rutilus rutilus lacustris*). The total of 68 most abundant metabolites are identified and quantified in the fish lenses and gills by the combination of LC-MS and NMR. It is shown that the concentrations of some compounds in the lens are much higher than that in the gills; that indicates the importance of these metabolites for the adaptation to the specific living conditions and maintaining the homeostasis of the fish lens. The lens metabolome undergoes significant seasonal changes due to the variations of dissolved oxygen level and fish feeding activity. The most season-affected metabolites are osmolytes and antioxidants, and the most affected metabolic pathway is the histidine pathway. In late autumn, the major lens osmolytes are *N*-acetyl-histidine and threonine phosphoethanolamine (Thr-PETA), while in winter the highest concentrations were observed for serine phosphoethanolamine (Ser-PETA) and *myo*-inositol. The presence of Thr-PETA and Ser-PETA in fish tissues and their role in cell osmotic protection are reported for the first time. The obtained concentrations can be used as baseline levels for studying the influence of environmental factors on fish health.

Keywords: freshwater fish; metabolomics; dissolved oxygen level; mass spectrometry; NMR spectroscopy

1. Introduction

A complete set of small-molecular-weight compounds in a tissue—a metabolome—reflects an actual state of the tissue and may significantly vary depending on the age, diet, and health status. The role of metabolomics in the study of human and animal pathogeneses rapidly increases [1–4]. The pathologic processes in a tissue are reflected in the metabolomic changes, causing the increase or decrease of the levels of certain metabolites. The metabolomic approach has proven its efficiency in environmental studies related to aquaculture. In particular, the metabolomic analysis of fish tissues has been successfully used for the study of the impact of external factors on fish health, including water contamination with pesticides [5], herbicides [6], aromatic hydrocarbons and mercury [7,8], low oxygen level [9], water temperature [10,11]. A recent review [12] is devoted to the application of the metabolomic approach to the study of viral, bacterial, and parasite fish diseases.

One can assume that metabolically active tissues—gills, blood, liver, meat—are more sensitive to environmental factors than relatively conservative tissues such as bones, lens, or vitreous humor. For that reason, the metabolically active fish tissues are often used for the analysis. On the other hand, the conservative tissues may accumulate the metabolomic changes induced by adverse ecological

factors or by diseases, and, therefore, give additional information on the mechanism of disease development. The metabolomic study of the fish lens attracts a special interest in the view of reports on extremely high cataract prevalence in farmed fish (especially salmonids) [13–15], in some cases reaching 100%. It has been suggested [11,16–18] that the disease cause is the low supply of amino acid histidine, used for the biosynthesis of the major osmolyte of the fish lens, *N*-acetyl-histidine (NAH) [19,20]. Indeed, low histidine level in the fish feed results in the low concentration of NAH in the eye lens; insufficient tissue buffering and osmoregulation causes the development of osmotic cataracts, especially after the seawater transfer [17].

The eye lens mostly consists of fiber cells without nuclei and organelles lost during the cell differentiation [21]. That makes the lens transparent in the visible light range, but the metabolic activity inside the lens is minimal. Therefore, the lens defense almost completely relies on small molecules either entering the lens from the surrounding aqueous humor (AH), or synthesized in metabolically active lens epithelial monolayer. First of all, these molecules include antioxidants preventing the development of oxidative stress, and osmolytes maintaining the intracellular pressure. Lack of antioxidants or osmoprotectants may lead to the damage of eye tissues, and to cataract development. The proper lens functioning also requires the constant supply of nutrients for cellular energy generation, biochemical synthesis, and other cellular functions.

It is important to notice that the majority of published metabolomic data are semi-quantitative, yielding the difference between the metabolomic profiles of experimental and control samples. The quantitative data on the metabolomic composition of fish tissues (metabolite concentrations in moles per gram of tissue) can be found only in a few papers for rather limited set of compounds. Recently, we developed an approach based on the combined application of NMR spectroscopy and liquid chromatography with mass-spectrometric and optical detection (LC-MS) to the quantitative metabolomic profiling of biological liquids and tissues [22–27]. This approach allows for the determining of concentrations of up to one hundred compounds in a sample. In the present paper, we apply this approach for the metabolomic profiling of lenses and gills of two kinds of freshwater fish—pike-perch (*Sander lucioperca*) and Siberian roach (*Rutilus rutilus lacustris*), inhabiting the basin of the Siberian river Ob. The major goals of the work are:

(a) To determine the major metabolites present in the fish lens and gill, including osmolytes, antioxidants, amino acids, organic acids etc., and to measure their concentrations;
(b) To compare the metabolomic profiles of the fish lens and gill. The gill is a very blood-rich tissue, while the metabolomic composition of AH surrounding the lens is very similar to that of blood plasma [22]. Therefore, the comparison of metabolomic compositions of the lens and gill may help to determine which compounds enter the lens from blood via AH, and which ones are specifically synthesized inside the lens;
(c) To compare the metabolomic composition of gills and lenses from herbivorous–omnivorous (*R. rutilus lacustris*) and predatory (*S. lucioperca*) fish;
(d) To compare the lens metabolomic composition of fish caught at different times of year in order to estimate the influence of a seasonal factor on the lens metabolomic profile.

2. Results

2.1. Metabolite Identification

Figures 1 and 2 show the NMR spectra of protein-free lipid-free extracts from the *S. lucioperca* lens and gill. Most of the signals in the NMR spectra correspond to well-known metabolites whose spectra are available in literature [6–9,24,26,28–30]. These metabolites include amino acids, organic acids, alcohols, sugars, nucleotides, and others. For the majority of these compounds, the identification was performed according to their NMR spectra without additional confirmation. In some cases, the signal assignment was unobvious; in these cases, the identification was confirmed by spiking the extract with commercial standard compounds.

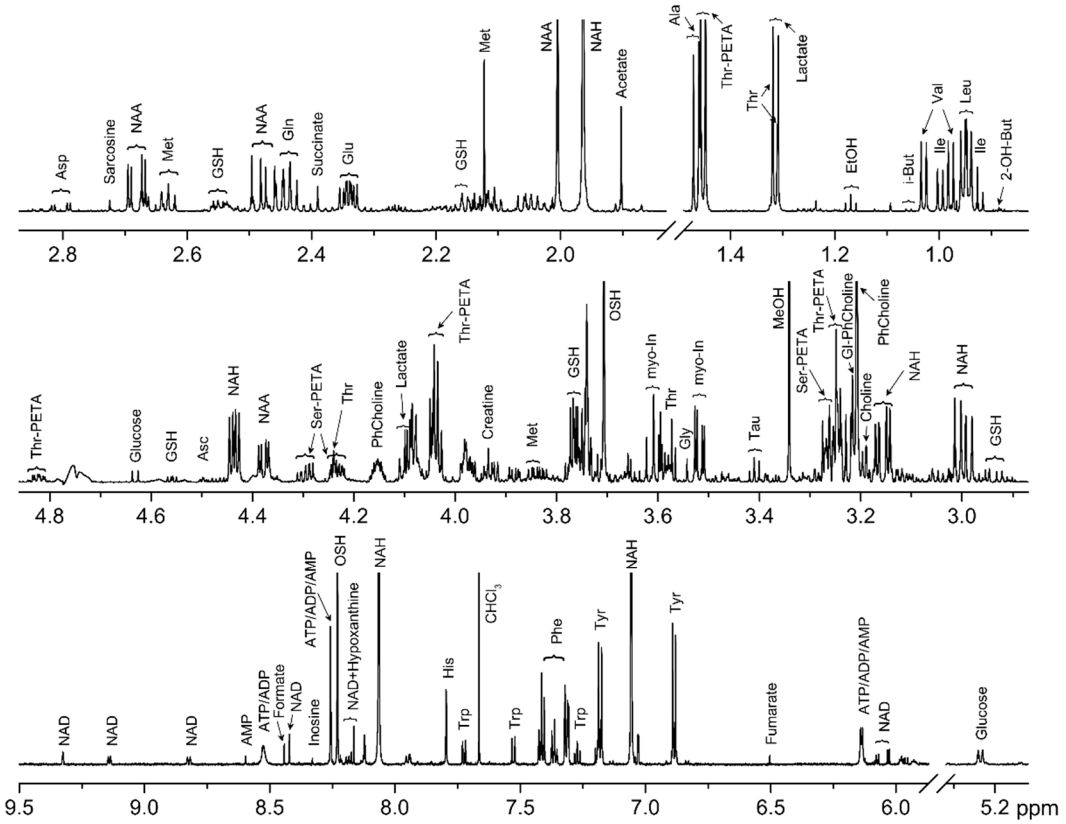

Figure 1. Representative ^{1}H NMR spectra of protein-free lipid-free extract from *S. lucioperca* lens with the metabolite assignment: 2-OH-But—2-hydroxy-butyrate; Gl-PhCholine—glycerophosphocholine; GSH—glutathione; i-But—isobutyrate; myo-In—*myo*-inositol; NAA—*N*-acetyl-aspartate; NAH—*N*-acetyl-histidine; OSH—ovothiol A; PETA—phosphoethanolamine; PhCholine—phosphocholine; Ser-PETA—serine phosphoethanolamine; Tau—taurine; Thr-PETA—threonine phosphoethanolamine. For amino acids and nucleotides, standard 3-letter symbols are used.

After preliminary metabolite identification, few major signals in the NMR spectra remained unassigned, including doublet at 1.45 ppm and 3 multiplets at 4.23 ppm, 4.30 ppm, 4.82 ppm. To assign these signals, the lens extract was chromatographically separated into 15 fractions, and each fraction was subjected to MS, MS/MS, and NMR analysis. That made it possible to identify two unknown metabolites, namely threonine phosphoethanolamine (Thr-PETA) and serine phosphoethanolamine (Ser-PETA). Quantitative analysis shows (see below) that these compounds are among the most abundant metabolites in the fish lens and gill. The chemical structures of these compounds are shown in Scheme 1, and their MS/MS and NMR properties are listed below.

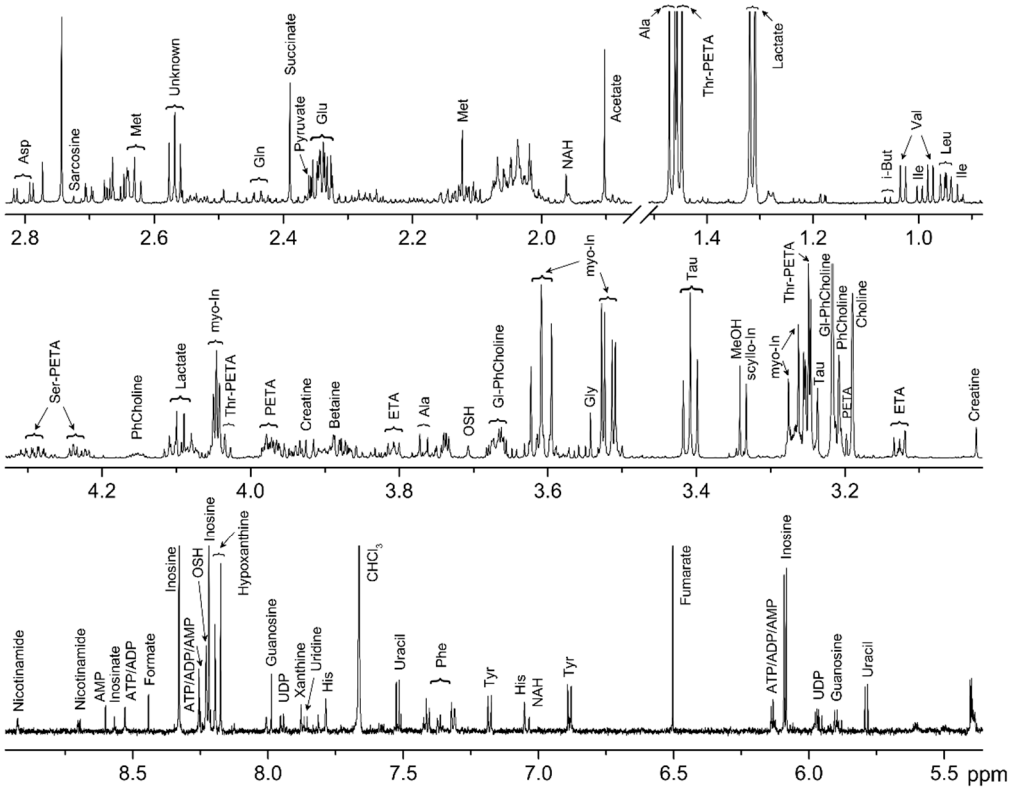

Figure 2. Representative ^{1}H NMR spectra of protein-free lipid-free extract from *S. lucioperca* gill with the metabolite assignment: ETA—ethanolamine; Gl-PhCholine—glycerophosphocholine; GSH—glutathione; i-But—isobutyrate; myo-In—*myo*-inositol; NAA—*N*-acetyl-aspartate; NAH—*N*-acetyl-histidine; OSH—ovothiol A; PETA—phosphoethanolamine; PhCholine—phosphocholine; scyllo-In—*scyllo*-inositol; Ser-PETA—serine phosphoethanolamine; Tau—taurine; Thr-PETA—threonine phosphoethanolamine. For amino acids and nucleotides, standard 3-letter symbols are used.

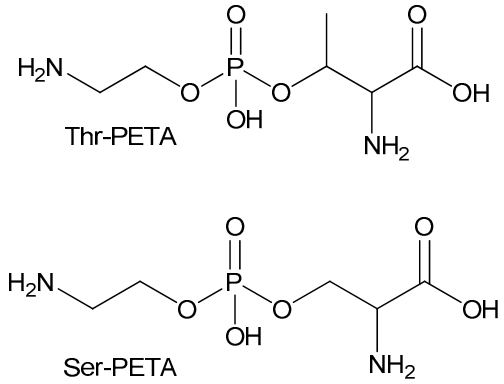

Scheme 1. Structures of Thr-PETA and Ser-PETA.

Thr-PETA:

^{1}H NMR (700 MHz, D_2O): 1.452 (3H, d, J = 6.7 Hz, CH_3); 3.247 (2H, m, CH_2); 3.736 (1H, dd, J = 2.2, 2.5 Hz, CH); 4.039 (2H, q, J = 5.3 Hz, CH_2); 4.820 (1H, m, CH).

MS/MS (ESI$^+$, 20.7 eV): 243.0737 [$C_6H_{16}N_2O_6P^+$], 200.0321 [$C_4H_{11}NO_6P^+$], 142.0269 [$C_2H_9NOP^+$], 120.0658 [$C_4H_{10}NO_3^+$], 102.0553 [$C_4H_8NO_2^+$], 98.9839 [$H_4O_4P^+$], 84.0446 [$C_4H_6NO^+$].

Ser-PETA:

^{1}H NMR (700 MHz, D_2O): 3.267 (2H, m, CH_2); 3.978 (1H, m, CH); 4.079 (2H, m, CH_2); 4.23 (1H, m, CH_2); 4.29 (1H, m, CH_2).

MS/MS (ESI$^+$, 20.5 eV): 229.0586 [$C_5H_{14}N_2O_6P^+$], 186.0166 [$C_3H_9NO_6P^+$], 166.0166 [$C_4H_9NO_4P^+$], 142.0267 [$C_2H_9NO_4P^+$], 106.0499 [$C_3H_8NO_3^+$], 98.9843 [$H_4O_4P^+$], 88.0396 [$C_3H_6NO_2^+$].

More detailed data on NMR and MS/MS characterization of Thr-PETA and Ser-PETA are presented in Supplementary Material (Figures S1–S4).

The annotation of signals in LC-MS spectra was performed by the search in online databases (HMDB, METLIN, ChemSpider, ChEBI) using the obtained exact m/z values and verified by the analysis on isotopic pattern, retention time, characteristic fragment or adduct ions, and MS/MS spectra. The compounds identified by LC-MS were checked by NMR data, and vice versa. For 26 compounds to be further quantified by LC-MS, solid verification (MSI guidelines level 1) was done by the injection of chemical standard samples. In the present work, only the metabolites quantified by NMR or LC-MS or by both methods were considered.

2.2. Metabolite Quantification

The measurements of metabolite concentrations were performed for tissues of *S. lucioperca* and *R. rutilus lacustris* caught in the Ob reservoir (Novosibirsk region, Siberia, Russia) during the late autumn (October–November) and winter (February) periods. Typically, ice freezes in Novosibirsk region in the second half of November, while ice-breaking occurs at the end of April. It is known that the level of dissolved oxygen (DO) in ice-covered lakes is maximal during the late autumn (before ice freezing), and minimal in winter due to the water isolation from atmosphere [31]. Therefore, the data on autumn fish correspond to high DO season, and on winter fish, to low DO season.

The concentrations of metabolites in lenses and gills were measured by two methods. The first method includes the integration of NMR signals in the spectra of tissue extracts relatively to the internal standard DSS followed by the recalculation of the metabolite concentration in the sample to the metabolite concentration in the tissue (in nmoles per gram of the tissue wet weight). The LC-MS-based quantification was performed using the external calibration curves constructed for each metabolite under study. The majority of metabolites were quantified using the NMR method, while LC-MS method was mostly used for metabolites whose NMR signals were strongly overlapped by signals of other compounds, or the concentrations were too low for the reliable NMR quantification. For additional control, the concentrations of several metabolites were measured by both NMR and LC-MS methods. The concentrations of a total of 68 metabolites present in the fish lens and gill have been determined. The results of the measurements are presented in Table 1, more detailed information can be found in Supplementary Material (Table S2). Table 1 also indicates which method was used for metabolite quantification, NMR or LC-MS. A symbol NMR* corresponds to metabolites, whose concentrations were measured by NMR and confirmed by LC-MS (both methods gave similar results). The metabolites in Table 1 are divided into six groups according to their chemical and biological properties and functionalities: “Amino acids”, “Organic acids”, “Alcohols, amines, and sugars”, ”Osmolytes”, “Antioxidants”, and “Nitrogenous bases, nucleotides, nucleosides”.

Table 1. Concentrations of metabolites in lenses and gills of *S. lucioperca* and *R. rutilus lacustris* caught in the Ob reservoir in late autumn and winter.

Metabolite	Method	*Sander lucioperca*			*Rutilus rutilus lacustris*		
		Lens Autumn, nmol/g	Lens Winter, nmol/g	Gill Winter, nmol/g	Lens Autumn, nmol/g	Lens Winter, nmol/g	Gill Winter, nmol/g
Amino acids							
Acetylcarnitine	NMR	30 ± 9	17 ± 2	16 ± 5	10 ± 4	18 ± 4	60 ± 30
Alanine	NMR	1600 ± 180	1500 ± 140	1200 ± 300	2300 ± 600	2100 ± 300	1800 ± 40
Asparagine	MS	30 ± 4	10 ± 1	6.7 ± 1.8	7.8 ± 1.6	4.9 ± 0.4	5.3 ± 2.7
Aspartate	NMR	280 ± 20	440 ± 40	190 ± 60	210 ± 60	200 ± 40	250 ± 80
Betaine	MS	6.2 ± 1.9	4.0 ± 0.7	240 ± 50	14 ± 7	11 ± 4	100 ± 40
Carnitine	MS	2.3 ± 0.3	0.70 ± 0.15	13 ± 2	12 ± 5	6.3 ± 2.7	31 ± 17
Creatine	NMR*	160 ± 40	73 ± 7	310 ± 40	130 ± 30	35 ± 6	1100 ± 200
Glutamate	NMR	2100 ± 200	2000 ± 140	1500 ± 200	2200 ± 200	1500 ± 130	2000 ± 200
Glutamine	NMR	1900 ± 200	990 ± 120	200 ± 30	2900 ± 540	3000 ± 100	630 ± 200
Glycine	NMR	130 ± 20	180 ± 40	660 ± 70	180 ± 80	230 ± 40	1400 ± 340
Histidine	NMR*	830 ± 70	330 ± 13	82 ± 17	350 ± 80	260 ± 20	170 ± 80
Isoleucine	NMR	550 ± 110	470 ± 60	88 ± 15	140 ± 50	60 ± 24	100 ± 80
Leucine	NMR	1600 ± 200	1400 ± 200	190 ± 30	890 ± 200	750 ± 170	250 ± 190
Lysine	MS	190 ± 70	52 ± 10	210 ± 40	90 ± 19	63 ± 20	660 ± 230
Methionine	NMR	710 ± 160	680 ± 160	130 ± 30	290 ± 80	220 ± 60	140 ± 70
N-Ac-3-Me-His	NMR	660 ± 220	76 ± 16	0	110 ± 40	44 ± 24	0
Ornithine	MS	46 ± 4	23 ± 5	50 ± 11	32 ± 6	18 ± 4	73 ± 15
Phenylalanine	NMR*	800 ± 190	440 ± 50	93 ± 13	240 ± 60	200 ± 40	130 ± 120
Proline	NMR*	81 ± 19	100 ± 30	190 ± 60	91 ± 16	65 ± 15	260 ± 180
Sarcosine	NMR	36 ± 10	13 ± 4	30 ± 7	4.3 ± 5.7	0	88 ± 30
Serine	NMR*	420 ± 130	720 ± 50	560 ± 80	2100 ± 300	2000 ± 150	1700 ± 1100
Threonine	MS	340 ± 130	320 ± 60	200 ± 40	420 ± 60	230 ± 60	180 ± 100
Tryptophan	NMR*	360 ± 120	380 ± 30	27 ± 6	170 ± 60	180 ± 30	14 ± 10
Tyrosine	NMR	1100 ± 400	780 ± 110	100 ± 20	450 ± 160	580 ± 170	160 ± 130
Valine	NMR*	790 ± 140	620 ± 90	190 ± 40	170 ± 50	93 ± 28	190 ± 130

Table 1. *Cont.*

Metabolite	Method	*Sander lucioperca*			*Rutilus rutilus lacustris*		
		Lens Autumn, nmol/g	Lens Winter, nmol/g	Gill Winter, nmol/g	Lens Autumn, nmol/g	Lens Winter, nmol/g	Gill Winter, nmol/g
Organic acids							
2-OH-butyrate	MS	34 ± 8	6.0 ± 2.3	2.7 ± 1.7	9.1 ± 4.8	1.5 ± 0.3	0.96 ± 0.81
AABA	NMR*	110 ± 25	53 ± 15	18 ± 3	180 ± 60	150 ± 27	46 ± 10
Acetate	NMR	510 ± 30	250 ± 20	170 ± 90	220 ± 60	180 ± 20	90 ± 40
Formate	NMR	60 ± 20	16 ± 8	26 ± 6	46 ± 32	65 ± 61	38 ± 26
Fumarate	NMR	16 ± 1	11 ± 3	94 ± 29	6.4 ± 3.3	4.3 ± 2.7	48 ± 12
GABA	MS	1.4 ± 0.9	0.49 ± 0.64	71 ± 18	12 ± 14	8.3 ± 4.9	460 ± 160
Isobutyrate	NMR	7.8 ± 2.4	0	6.9 ± 3.2	0	0	9.4 ± 5.0
Lactate	NMR	2500 ± 500	1000 ± 200	3400 ± 600	1700 ± 600	1500 ± 140	5100 ± 1900
Pyroglutamate	MS	94 ± 8	78 ± 15	75 ± 34	72 ± 11	65 ± 5	29 ± 15
Pyruvate	NMR	0	10 ± 2	43 ± 14	5.5 ± 6.6	11 ± 3	23 ± 8
Succinate	NMR	90 ± 15	59 ± 8	87 ± 40	34 ± 7	34 ± 8	59 ± 50
Alcohols, amines, and sugars							
Choline	NMR	120 ± 20	140 ± 30	970 ± 200	43 ± 9	86 ± 25	400 ± 80
ETA	NMR	0	0	1500 ± 200	0	0	620 ± 440
Glucose	NMR	290 ± 120	140 ± 20	320 ± 200	540 ± 400	250 ± 90	1600 ± 1600
Glycerol	NMR	50 ± 6	73 ± 18	530 ± 130	0	0	300 ± 200
Gl-PhCholine	NMR	260 ± 30	340 ± 40	1800 ± 400	95 ± 26	56 ± 8	1400 ± 400
PhCholine	NMR	1500 ± 200	810 ± 60	520 ± 170	2200 ± 200	1300 ± 50	610 ± 160
PETA	NMR*	630 ± 230	250 ± 43	1700 ± 300	350 ± 60	560 ± 130	2500 ± 700
scyllo-Inositol	NMR	10 ± 3	130 ± 40	280 ± 70	11 ± 3	13 ± 11	58 ± 30
Osmolytes							
myo-Inositol	NMR	2100 ± 400	7300 ± 700	8200 ± 1100	2300 ± 400	5200 ± 1900	2000 ± 500
NAA	NMR	3300 ± 500	2000 ± 200	130 ± 100	560 ± 70	490 ± 70	30 ± 10
NAH	NMR	8300 ± 600	2300 ± 400	50 ± 20	6800 ± 400	3800 ± 300	13 ± 5
Ser-PETA	NMR	2300 ± 600	3200 ± 400	3300 ± 500	6700 ± 600	5600 ± 400	3800 ± 1100
Taurine	NMR	340 ± 80	480 ± 110	5500 ± 780	370 ± 200	170 ± 30	8700 ± 1200
Thr-PETA	NMR	4400 ± 300	2600 ± 500	1600 ± 300	4100 ± 900	1600 ± 500	1400 ± 600

Table 1. *Cont.*

Metabolite	Method	*Sander lucioperca*			*Rutilus rutilus lacustris*		
		Lens Autumn, nmol/g	Lens Winter, nmol/g	Gill Winter, nmol/g	Lens Autumn, nmol/g	Lens Winter, nmol/g	Gill Winter, nmol/g
Antioxidants							
Ascorbate	NMR	91 ± 17	40 ± 7	23 ± 11	54 ± 10	57 ± 8	100 ± 180
GSH	NMR*	470 ± 150	490 ± 80	17 ± 15	280 ± 130	150 ± 100	100 ± 140
GSSG	NMR*	260 ± 80	200 ± 30	70 ± 20	140 ± 60	37 ± 17	92 ± 46
OSH	NMR	3000 ± 200	1600 ± 108	220 ± 70	1100 ± 200	270 ± 80	100 ± 90
Nitrogenous bases, nucleotides, nucleosides							
CMP	MS	17 ± 2	6.5 ± 0.3	18 ± 5	39 ± 4	20 ± 3	20 ± 5
ADP	NMR	230 ± 20	120 ± 10	49 ± 10	220 ± 40	150 ± 10	85 ± 65
AMP	NMR*	59 ± 9	57 ± 17	20 ± 16	53 ± 16	57 ± 6	55 ± 50
ATP	NMR	930 ± 60	540 ± 40	22 ± 5	840 ± 60	560 ± 80	230 ± 240
Creatinine	NMR	13 ± 6	7.8 ± 1.6	15 ± 5	19 ± 6	28 ± 9	34 ± 9
Guanosine	NMR	0	0	77 ± 12	0	0	6.0 ± 4.4
Hypoxanthine	NMR	0	0	290 ± 80	0	0	300 ± 250
Inosinate	NMR	12 ± 2	23 ± 6	21 ± 12	38 ± 16	66 ± 19	64 ± 69
Inosine	NMR	28 ± 4	19 ± 5	600 ± 70	0	0	80 ± 50
NAD	NMR	180 ± 30	81 ± 10	1.8 ± 0.9	100 ± 30	46 ± 9	6.7 ± 9.9
Nicotinamide	NMR*	3.4 ± 0.7	1.9 ± 0.6	48 ± 6	2.7 ± 0.3	3.9 ± 1.3	39 ± 14
Uracil	NMR	0	0	190 ± 30	0	0	160 ± 90
Uridine	MS	4.6 ± 0.7	3.1 ± 1.3	36 ± 5	3.3 ± 1.6	3.8 ± 1.6	43 ± 27
Xanthine	NMR	0	0	56 ± 14	0	0	130 ± 110

NMR*—concentrations were measured by NMR and confirmed by LC-MS. List of abbreviations: 2-OH-Butyrate—2-hydroxy-butyrate; AABA—α-Aminobutyrate; Acetylcarnitine—*N*-acetyl-carnitine; ETA—ethanolamine; GABA—γ-aminobutyrate; Gl-PhCholine—glycerophosphocholine; GSH—glutathione; GSSG—glutathione oxidized; i-But—isobutyrate; myo-In—myo-inositol; *N*-Ac-3-Me-His—*N*-acetyl-3-methyl-histidine; NAA—*N*-acetyl-aspartate; NAH—*N*-acetyl-histidine; OSH—ovothiol A; PETA—phosphoethanolamine; PhCholine—phosphocholine; Ser-PETA—serine phosphoethanolamine; Thr-PETA—threonine phosphoethanolamine. For nucleotides, standard 3-letter symbols are used.

2.3. Quantitative Data Analysis

To get the overview of the general metabolomic differences between the four lens groups, the data on metabolite concentrations in lenses were subjected to a principal component analysis (PCA). The following groups were analyzed: lenses from *S. lucioperca* caught in autumn and in winter, and lenses from *R. rutilus lacustris* caught in autumn and in winter. Figure 3 (left panel) shows the PCA scores plot for the 1st principal component (PC1 = 45.1% of explained variance) versus the 2nd component (PC2 = 25.8% of explained variance). The corresponding loadings plot is presented in Figure 3 (right panel).

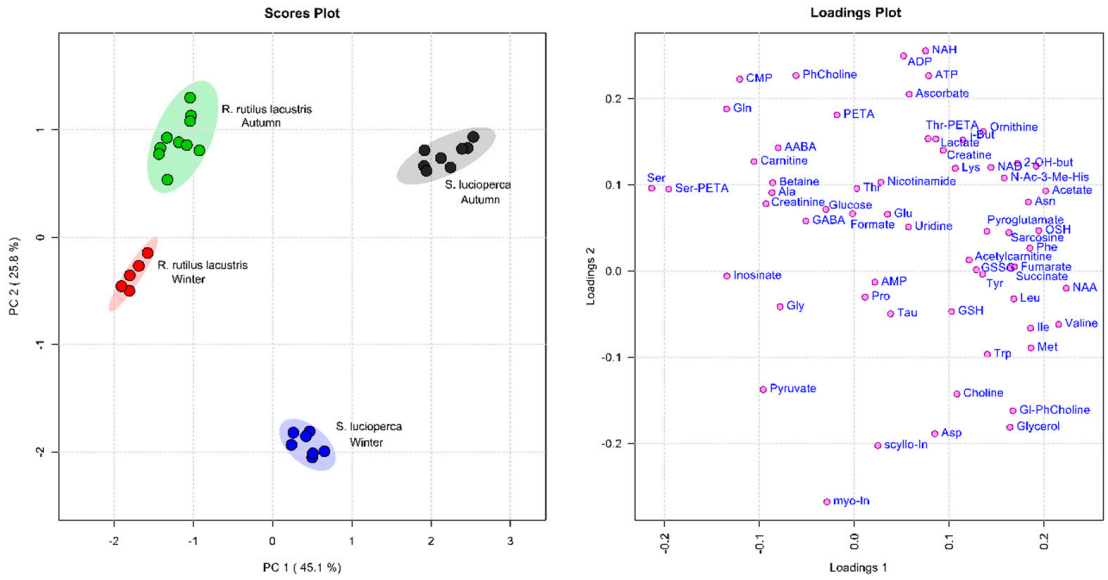

Figure 3. Scores (**left**) and loadings (**right**) plots of principal component analysis (PCA) of lens metabolomic profiles of *S. lucioperca* caught in autumn (black) and winter (blue) periods and *R. rutilus lacustris* caught in autumn (green) and winter (red) periods. The data are range scaled. Colored ovals indicate 95% confidence regions. Variance explained by the first (PC1) and second (PC2) principal components are indicated on the axis of scores plot.

The data in the PCA scores plot are concentrated into four distinct groups, which demonstrates that: (a) the metabolomic compositions of *S. lucioperca* and *R. rutilus lacustris* lenses differ significantly, and the genera are separated along the PC1 axis; (b) the metabolomic profiles of lenses from both fish genera undergo noticeable seasonal variations spread along the PC2 axis; (c) within each experimental group, the data scattering is rather small.

Figure 4 shows boxplots for concentrations of nine metabolites which demonstrate the most significant differences between genera and the most pronounced seasonal variations. *myo*-Inositol, NAH, Thr-PETA are the most discriminative metabolites between genera, and they demonstrate significant seasonal dependences (Figure 3). Large seasonal variations are also observed for ADP, histidine, *N*-acetyl-aspartate (NAA), OSH, serine, and Ser-PETA.

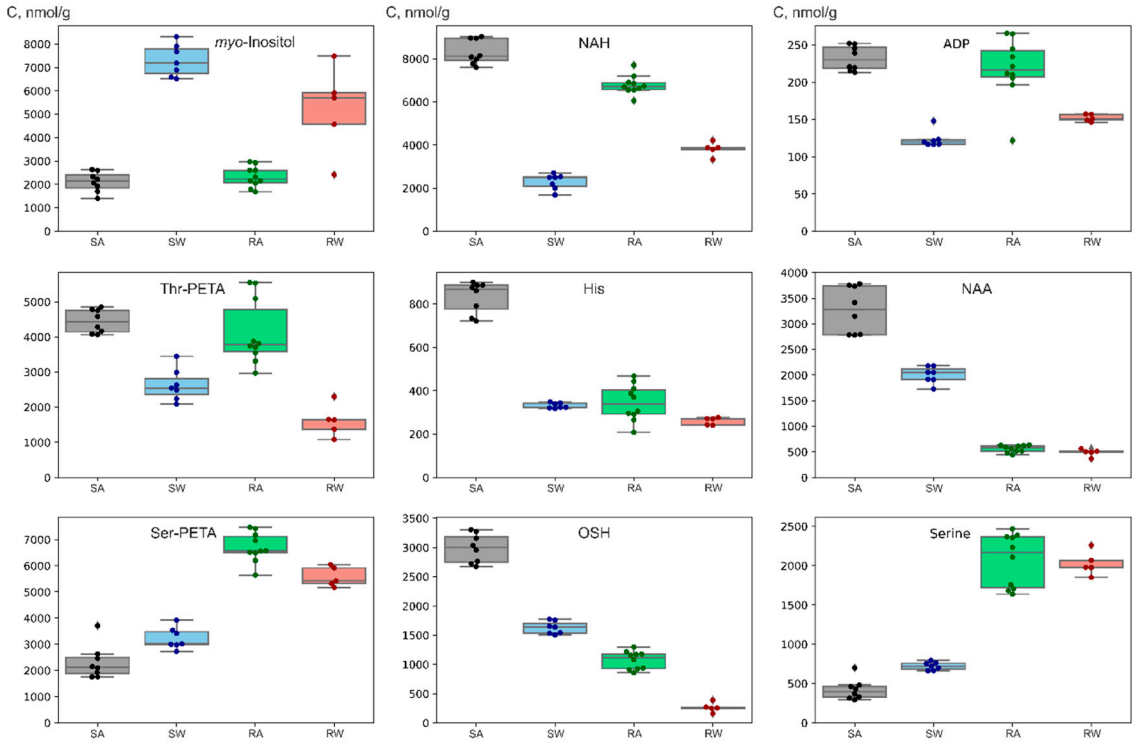

Figure 4. Boxplots for concentrations of metabolites in lenses of *S. lucioperca* caught in autumn (SA, black) and winter (SW, blue) periods, and *R. rutilus lacustris* caught in autumn (RA, green) and winter (RW, red) periods.

The differences in the metabolite concentrations in the fish lens and gill were calculated as the ratio of averaged concentrations in the lens to that in the gill (lens/gill ratio). To reveal statistically important differences between the groups, the Mann–Whitney *U*-test (with the use of FDR correction) was performed. The resulting barplots containing graphical information on the lens/gill ratios are presented in Figure 5 (left panel for *S. lucioperca* and right panel for *R. rutilus lacustris*). Only the metabolites which differ significantly ($p < 0.05$, fold change > 1.5) are shown. Numerical values can be found in Supplementary Material (Table S3). The bars expanding to the left from the unity correspond to the elevated level of a metabolite in the gill, and to the right, to the elevated level in the lens. For several metabolites the ratio of their levels in lens to that in the gill (or vice versa) exceeds two orders of magnitude. For the majority of such values that means that a metabolite was not detected in either gill or lens, correspondingly. In fact, the numerical ratio of two significantly different values is rather unreliable; therefore we decided to cut all bars at the level of the lens/gill and gill/lens ratios equal to 30. The lenses of both fish types contain elevated levels of NAH, *N*-acetyl-3-methyl-histidine (*N*-Ac-3-Me-His), NAA, NAD, and tryptophan, while the reduced concentrations (as compared to gills) are observed for xanthine, uracil, hypoxanthine, guanosine, ethanolamine (ETA), isobutyrate, γ-aminobutyrate (GABA), and inosine.

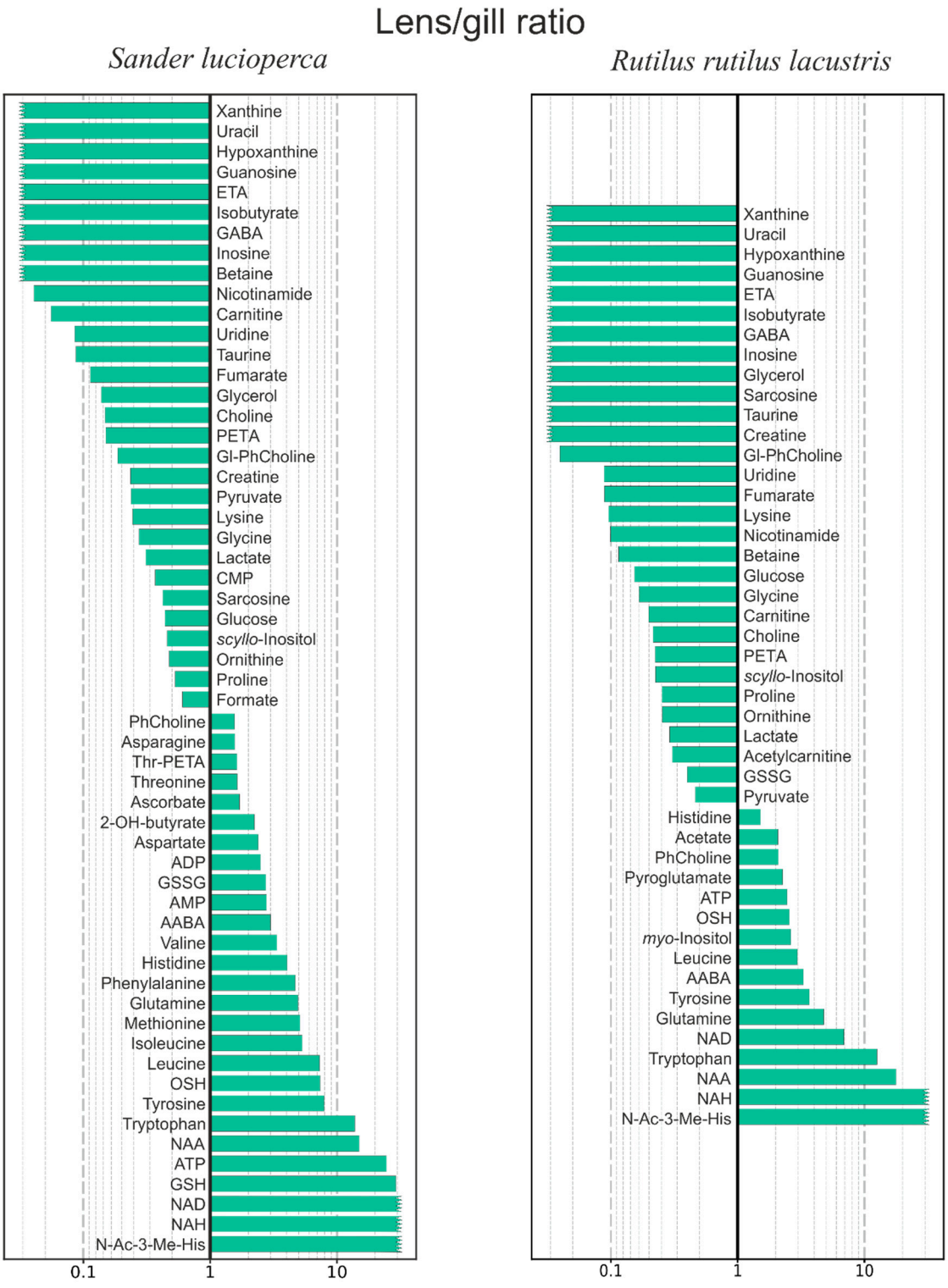

Figure 5. Barplots for statistically significant differences ($p < 0.05$) in the metabolomic content of lenses and gills. Bars show the ratio of metabolite concentrations in lenses to that in gills for *S. lucioperca* (**left**) and *R. rutilus lacustris* (**right**) in logarithmic scale. Jagged bar ends indicate ratios >30 and <0.03. The metabolites with insignificant difference (fold change below 1.5, $p > 0.05$) between lens and gill are not shown. The bars expanding to the left from the unity correspond to the elevated level of a metabolite in the gill, and to the right, to the elevated level in the lens.

For further investigation of pathways involved in the seasonal variations occurring in the fish lens, we performed quantitative metabolite set enrichment analysis (MSEA), comparing the metabolite concentrations in autumn and in winter. The assignment of metabolites to particular pathways was performed with the use of MetaboAnalyst web platform [32] using self-defined metabolite sets based on the SMPDB (Small Molecule Pathway Database) library as described in the Materials and Methods section. The results of MSEA are presented in Figure 6 (left panel for *S. lucioperca* and right panel for *R. rutilus lacustris*) and in Supplementary Material (Table S4). The "Histidine metabolism" pathway was modified by addition of NAH, OSH, and their intermediate compounds to the list of metabolites already existing in the SMPDB library; an asterisk sign (*) indicates this modification. The "Histidine metabolism*" is the most season-affected pathway for both genera. The following pathways are also amongst the most affected in both genera: "Citric acid cycle", "Arginine and proline metabolism". Besides, in *S. lucioperca* pronounced changes are observed in "Ammonia recycling", "Galactose metabolism", and "Inositol metabolism". For *R. rutilus lacustris*, the "Phospholipid biosynthesis", "Phenylalanine and tyrosine metabolism", and "Cysteine metabolism" are amongst the most affected pathways.

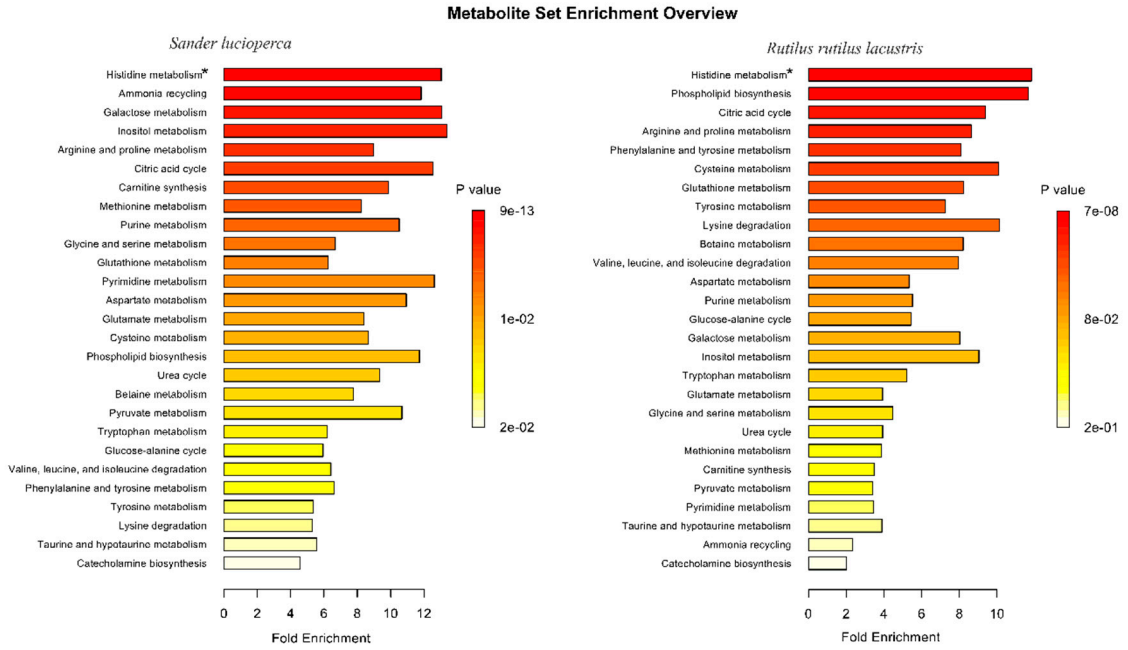

Figure 6. Metabolite set enrichment analysis based on the comparison of metabolite concentrations in lenses of autumn and winter *S. lucioperca* (**left**) and *R. rutilus lacustris* (**right**).

2.4. Metabolite Group Analysis

The information presented in the Table 1 and Figures 3–6 was used for the analysis of the metabolite concentrations in the lenses and gills of *S. lucioperca* and *R. rutilus lacustris*. The main objectives of the analysis were to establish the most abundant metabolites in tissues and to reveal similarities and differences between sample groups.

2.4.1. Amino Acids

Alanine and glutamine are the most abundant amino acids (with the exception of taurine which was placed in the group "Osmolytes") in lenses and gills of both *S. lucioperca* and *R. rutilus lacustris*.

The amino acid compositions of gills of *S. lucioperca* and *R. rutilus lacustris* are rather similar. Noticeable differences (by a factor of ca. 3) were observed for glutamine, lysine, serine, sarcosine, creatine, carnitine, and *N*-acetyl-carnitine; for all these amino acids, their concentrations in the *R. rutilus*

lacustris gills were higher. The only amino acids prevailing in the *S. lucioperca* gills are tryptophan and betaine.

The levels of the majority of amino acids in lenses of *S. lucioperca* and *R. rutilus lacustris* are also similar. The concentrations of valine, isoleucine, methionine, asparagine, phenylalanine, *N*-Ac-3-Met-His, and sarcosine are higher in the *S. lucioperca* lens, while the concentrations of serine, carnitine, and betaine—in the *R. rutilus lacustris* lens.

The comparison of amino acid compositions of the fish gills and lens (Figure 5) shows that the lens contains elevated levels of leucine, methionine, glutamine, tyrosine, histidine, phenylalanine, and tryptophan. The concentration of the latter in lenses is higher than that in the gills by an order of magnitude. The reduced concentrations in lenses as compared to gills were observed for lysine, glycine, proline, sarcosine, creatine, carnitine, and betaine.

2.4.2. Organic Acids

The organic acids listed in Table 1 are mostly intermediates or final products of metabolic reactions. Since the metabolism in the gill is much more active than that in the lens, the concentrations of the majority of organic acids in the gill are higher than in the lens. Especially high gill/lens ratios were found for GABA and fumarate. The prevalence in the lens was observed only for two acids, 2-hydroxy-butyrate and α-aminobutyrate (AABA). Lactate, being the final glycolysis product, is by far the most abundant acid in the fish lens and gills. For the majority of organic acids, their levels in the lens in autumn are higher than in winter.

2.4.3. Alcohols, Amines, and Sugars

Similarly to organic acids, the levels of the majority of metabolites from this group in gills are much higher than that in lenses, with the only exception of phosphocholine. The lowest levels in lenses as compared to gills were observed for ethanolamine, choline, and glycerol.

2.4.4. Osmolytes

The most abundant compound in the *S. lucioperca* gills is *myo*-inositol (8.2 μmol/g) followed by taurine (5.5 μmol/g) and Ser-PETA (3.3 μmol/g). Apparently, one of the major roles of these metabolites in the fish blood and gill tissue is the cellular osmotic protection. Thr-PETA (1.6 μmol/g) most likely also participates in the osmotic protection. The same compounds play the role of osmoprotectants also in the *R. rutilus lacustris* gills, but their abundances differ: The most abundant metabolite is taurine (8.7 μmol/g) followed by Ser-PETA (3.8 μmol/g), *myo*-inositol (2.0 μmol/g), and Thr-PETA (1.4 μmol/g).

The major osmolytes in the fish lens differ significantly from that in the fish gill. Firstly, the concentrations of taurine in lenses (0.2–0.5 μmol/g) are much smaller than in gills. Secondly, the lens contains high concentrations of *N*-acetyl-histidine (NAH) and *N*-acetyl-aspartate (NAA). Thus, the full list of the major osmolytes in the lens of both *S. lucioperca* and *S. lucioperca* includes *myo*-inositol, Thr-PETA, Ser-PETA, NAH, and NAA. However, the abundances of these metabolites in lenses of *S. lucioperca* and *R. rutilus lacustris* differ, and their levels undergo significant seasonal changes. In lenses of autumn *S. lucioperca*, the most abundant osmolytes are NAH and Thr-PETA followed by NAA, Ser-PETA, and *myo*-inositol. During the winter, the levels of NAH, Thr-PETA, and NAA decrease, while the concentrations of Ser-PETA and *myo*-inositol increase. As a result, in winter, Ser-PETA and *myo*-inositol become the most abundant osmolytes in the *S. lucioperca* lens (Table 1). Similar seasonal changes occur in the lens of *R. rutilus lacustris*: NAH, Ser-PETA, and Thr-PETA prevail in autumn, while Ser-PETA and *myo*-inositol—in winter.

2.4.5. Antioxidants

In gills of *R. rutilus lacustris*, three major antioxidants—ovothiol A (1-methyl-4-thiol-L-histidine, OSH), glutathione (GSH), and ascorbate—are present in similar concentrations of approximately 100 nmol/g. In gills of *S. lucioperca*, the level of OSH is two times higher, while the levels of GSH

and ascorbate are significantly lower. Ergothioneine was detected (but not quantified) only in gills of *R. rutilus lacustris*.

The concentration of OSH in lenses of both *S. lucioperca* and *R. rutilus lacustris* is significantly higher than in gills. Especially high levels of OSH were detected in lenses of autumn fish—3 μmol/g for *S. lucioperca* and 1.1 μmol/g for *R. rutilus lacustris*. In winter, the levels of OSH in lenses significantly drop (two-fold for *S. lucioperca* and four-fold for *R. rutilus lacustris*). The seasonal variations of GSH in the lens are less pronounced: practically no changes were found for *S. lucioperca*, and approximately a two-fold decrease in winter for *R. rutilus lacustris*. The level of ascorbate varies in the fish lens from 30 to 100 nmol/g, ergothioneine in lenses was not detected.

2.4.6. Nitrogenous Bases, Nucleotides, Nucleosides

Most of compounds in this group are the products of intracellular biosynthesis, so one can expect that their concentrations in a tissue depend on the metabolic activity. Indeed, lens/gill ratio >1 was found only for ATP, ADP, AMP, and NAD. No significant differences were found between tissues of *S. lucioperca* and *R. rutilus lacustris*, the seasonal variations of the lenticular levels for the majority of metabolites from this group are also minimal.

3. Discussion

The present work is the first report on the detailed quantitative metabolomic composition of the fish tissues. Measurements were performed for lenses and gills from two types of freshwater fish—*S. lucioperca* and *R. rutilus lacustris*. The gill is a metabolically active blood-rich tissue, while the metabolic activity inside the lens is minimal. Although the metabolome is implicitly transient, the intracellular metabolites can stay inside the anatomically isolated tissue (such as the eye lens) for a long time. Thus, one can expect that the metabolomic composition of the gills reacts to the external factors promptly but reversibly, while the metabolomic changes in the lens accumulate with time. The obtained data were used for the comparison of metabolomic profiles of the lens and gill belonging to the same fish; study of seasonal variations of the lens metabolomic composition; the comparison of the metabolomic composition of tissues belonging to herbivorous–omnivorous (*R. rutilus lacustris*) and predatory (*S. lucioperca*) fishes.

The comparison of metabolomic profiles of fish gills shows that the levels of the majority of amino acids in *R. rutilus lacustris* gills are higher than that in *S. lucioperca* gills. *R. rutilus lacustris* gills also contain higher concentrations of AABA, GABA, glucose, ascorbate, GSH, AMP, and NAD. Most likely, the observed difference should be attributed to the different types of food of omnivorous and predatory fishes. In lenses, one can see a different picture: The concentrations of many metabolites in the *S. lucioperca* lens are significantly higher than in the *R. rutilus lacustris* lens. These metabolites include amino acids (isoleucine, methionine, sarcosine, valine), osmolytes (NAA), antioxidants (GSH and OSH). The amino acids are ingested with food, while NAA, GSH, and OSH are the products of intracellular biosynthesis. Therefore, it is doubtful whether the difference in the lens metabolomic compositions of *S. lucioperca* and *R. rutilus lacustris* corresponds to the different types of food only—more likely, the difference also originates from the different contributions of metabolic pathways formed during the evolution of two fish genera.

There are a significant number of metabolites whose concentrations in the gills are rather high, while their lenticular levels are either low or were not detected at all. The most significant difference in concentrations between gills and lens was found for GABA, ETA, isobutyrate, taurine, and a group of nitrogenous bases and nucleosides: inosine, guanosine, xanthine, hypoxanthine, uracil, uridine (Figure 5). It is known that the metabolomic composition of the blood plasma is very similar to that of aqueous humor surrounding the lens and providing the lens nutrition and waste removal [22]. Therefore, the majority of these compounds should be attributed to the intracellular metabolites of the gills tissue and blood. In the lens cells the metabolic activity is low, and these compounds are either not produced or produced in much lower amounts.

On the other hand, there are lens-specific compounds whose levels in the lens are significantly higher than in the gill. These metabolites include lenticular osmolytes NAH and NAA, and antioxidants OSH and GSH. Most likely, these compounds are synthesized in metabolically-active lens epithelial cells for the lens protection against osmotic and oxidative stresses. Surprisingly, the lens also contains an enhanced level of ATP despite the low metabolic activity in the lens cells. It can be assumed that the high lenticular ATP level corresponds to either activity of Na^+/K^+ pumps governing the water circulation through the lens [33–35] or to the mitochondrial activity taking place in the lens epithelial layer and outer cortex, and providing very low oxygen concentration in the inner parts of the lens [36].

There are three major seasonal factors which can affect the metabolomic composition of the fish tissues: the water temperature, the DO level, and the fish feeding activity. In the present study, the temperature factor is excluded: The water temperatures in late autumn and winter are similar, 4–7 °C. Low DO level during the winter leads to the deceleration of metabolic processes in fish. The metabolomic composition of the fish lens undergoes significant seasonal changes due to the low DO level and low feeding activity in winter. The most pronounced decrease of the lenticular level in winter was observed for amino acids creatine, glutamine, histidine, and *N*-Ac-3-Me-His; for the majority of organic acids; for osmolytes NAH and Thr-PETA; for antioxidant OSH. The winter decrease of organic acid levels in the fish lens probably reflects the deceleration of metabolic reactions, and, correspondingly, the lower rate of the generation of metabolic products.

To the best of our knowledge, till now NAH was the only well-recognized osmolyte in the fish lens [19,20]. In the present work, we have shown that several compounds protect the lens cells from the osmotic stress: *myo*-inositol, Thr-PETA, Ser-PETA, NAH, and NAA. In this regard, the fish lens significantly differs from mammalian lenses: For example, the major osmolytes in the rat lens are taurine and hypotaurine [25], and in the human lens—*myo*-inositol [24,30]. The list of osmolytes in the fish lens also differs from that in the fish gill, where high level of taurine was observed, while NAH is present in rather low concentration. The complex composition of osmolytes in the fish lens is probably an evolutionary response to the seasonal variations of the environment: During the periods of low oxygen content in the water and low feeding activity, the histidine supply may become insufficient for NAH synthesis, and the lens osmotic protection relies on other metabolites, such as *myo*-inositol and Ser-PETA. In this work, the presence of Thr-PETA and Ser-PETA in the fish tissues and their role in the cell osmotic protection are reported for the first time.

In the vast majority of animal tissues, GSH, ergothioneine, and ascorbate are the main antioxidants providing the deactivation of free radicals and the reduction of oxidized molecules [37–39]. Our lab has recently reported the finding of high concentrations of OSH in the fish lens [26]. The results of this work confirm that the major antioxidant of the fish lens is OSH. OSH is one of the strongest antioxidants existing in nature: Since pKa value of the thiol group is very low (pKa ≈ 1.0–1.4 [40–43], under physiological conditions OSH exists predominantly in highly reactive thiolate form. For that reason, the oxidation potential of OSH is significantly lower than that of GSH [44], and the oxidation of OSH by electron acceptors proceeds with the higher rate constants than that for GSH [40,45]. Earlier, OSH and its methylated derivatives were found in eggs and ovarian tissue of marine invertebrates (such as sea urchin, sea star, scallop, octopus) [46–49]. It was supposed [26] that in the fish lens, OSH represents the first line of the cellular defense against oxidative stress, reducing reactive oxygen species. Oxidized ovothiol molecules OSSO are then reduced by GSH [50], and oxidized glutathione GSSG is reduced by glutathione reductase. This reaction scheme might explain high concentrations of NAD in the fish lens, since the enzymatic reduction of GSSG requires the participation of NAD(P)H in the reaction.

OSH was also detected in the fish gills. Its level in the gill is much lower than in the lens; nevertheless, the concentration of OSH in the gill is similar or higher than the concentration of GSH. Therefore, one can assume that OSH plays an important role as an intracellular antioxidant not only in the lens, but also in other fish tissues.

The results of this work point to the importance of histidine supply in fish food. This amino acid is used for biosynthesis of two metabolites playing a vital role in maintaining homeostasis in the fish lens—the main lens osmolyte NAH and the main lens antioxidant OSH. Low feeding activity and deceleration of metabolic processes in winter cause a drop in lenticular levels of histidine, NAH, and OSH. The NAH deficiency can be compensated by synthesis of other osmolytes (*myo*-inositol and Ser-PETA), but the lack of OSH makes the lens tissue significantly more vulnerable to the oxidative stress. In particular, several publications [10,13,15,16,18] reported that the low dietary histidine supplementation provokes the cataractogenesis in farmed salmon, which was attributed to the decrease of the NAH level in the lens and the development of osmotic cataract. It is possible that the lack of OSH in the lens also makes a significant contribution to cataract development.

4. Materials and Methods

4.1. Chemicals

Chloroform, methanol, and acetonitrile (HPLC grade) were purchased from Panreac (Barcelona, Spain). D_2O 99.9% was purchased from Armar Chemicals (Dottingen, Switzerland). All other chemicals were purchased from Sigma-Aldrich (St. Louis, MO, USA). H_2O was deionized using Ultra Clear UV plus TM water system (SG water, Hamburg, Germany) to the quality of 18.2 MOhm.

4.2. Fish Sample Collection

The study was conducted in accordance with the ARVO Statement for the Use of Animals in Ophthalmic and Vision Research and the European Union Directive 2010/63/EU on the protection of animals used for scientific purposes, and with the ethical approval from the International Tomography Center (ECITC-2017-02). No special permission from the national or local authorities is required.

Pike-perch (*Sander lucioperca*, body weight 200–300 g) and Siberian roach (*Rutilus rutilus lacustris*, body weight 80–110 g) were caught in the Ob reservoir: *S. lucioperca*—in October (n = 8) and February (n = 7); *R. rutilus lacustris*—in November (n = 10) and February (n = 8). The exact dates and conditions of catching are given in Supplementary Material (Table S1). The fish were killed with a concussive blow to the head immediately after the catching, the lenses and gills were cut from the fish, frozen and kept at −70 °C until analyzed.

4.3. Fish Lens and Gill Preparation

Each fish lens was weighed prior to homogenization: for *S. lucioperca*, the typical lens weight was 100 mg, and for *R. rutilus lacustris*—40 mg. Only one lens from each fish was used for the analysis. The lens was placed in a glass vial and homogenized with a TissueRuptor II homogenizer (Qiagen, Netherlands) in 1600 µL of cold (−20 °C) MeOH, and then, 800 µL of water and 1600 µL of cold chloroform were added. The mixture was shaken well in a shaker for 20 min and left at −20 °C for 30 min. Then the mixture was centrifuged at 16,100× g, +4 °C for 30 min, yielding two immiscible liquid layers separated by a protein layer. The upper aqueous layer (MeOH-H_2O) was collected, divided into two parts for NMR (2/3) and LC-MS (1/3) analyses, and lyophilized.

Each fish gill was divided into arch and filaments. Only gill filaments were used for the analysis. Samples were weighed prior to homogenization: for *S. lucioperca*, the typical gill filament weight was 95 mg, and for *R. rutilus lacustris*—110 mg. The homogenization and extraction procedures for gill filaments were performed in the same way as for fish lenses.

4.4. NMR Measurements

The extracts for NMR measurements were re-dissolved in 600 µL of D_2O containing 6×10^{-6} M sodium 4,4-dimethyl-4-silapentane-1-sulfonic acid (DSS) as an internal standard and 20 mM deuterated phosphate buffer to maintain pH 7.2.

The ^{1}H NMR measurements were carried out at the Center of Collective Use «Mass spectrometric investigations» SB RAS on a NMR spectrometer AVANCE III HD 700 MHz (Bruker BioSpin, Rheinstetten, Germany) equipped with a 16.44 Tesla Ascend cryomagnet. The proton NMR spectra for each sample were obtained with 96 accumulations. Temperature of the sample during the data acquisition was kept at 25 °C, the detection pulse was 90 degree. The repetition time between scans was 20 s to allow for the relaxation of all spins. Low power radiation at the water resonance frequency was applied prior to acquisition to presaturate the water signal. The concentrations of metabolites in the samples were determined by the peak area integration respectively to the internal standard DSS.

4.5. LC-MS Measurements

The extracts for LC-MS analysis were re-dissolved in 100 µL of aqueous solution containing 10 µM *N*-acetyltryptophanamide as an internal control. For each sample, three dilutions (1, 1/4, 1/16) were made to extend the coverage of metabolite concentrations.

The LC separation was performed on a UltiMate 3000RS chromatograph (Dionex, Germering, Germany) using a hydrophilic interaction liquid chromatography (HILIC) method on a TSKgel Amide-80 HR (Tosoh Bioscience, Griesheim, Germany) column (4.6 × 250 mm, 5 µm) as described earlier [26]. The chromatograph was equipped with a flow cell diode array UV-vis detector (DAD) with 190–800 nm spectral range. Solvent A consisted of 0.1% formic acid solution in H_2O, solvent B consisted of 0.1% formic acid solution in acetonitrile. The gradient was (solvent B): 95% (0–5 min), 95%–65% (5–32 min), 65%–35% (32–40 min), 35% (40–48 min), 35%–95% (48–50 min), 95% (50–60 min); the flow rate was 1 mL/min, the sample injection volume was 10 L. After the DAD cell, a home-made flow splitter (1:10) directed the lesser flow to an ESI-q-TOF high-resolution hybrid mass spectrometer maXis 4G (Bruker Daltonics, Bremen, Germany). The mass spectra were recorded in a positive mode with 50–1000 m/z range. The MS setup, the calibration procedure, and the data processing were described in detail earlier [25–27,51]. Briefly, eight solutions containing an equimolar mixture of 26 metabolites with the concentrations ranging from 43.5 to 87 µM were subjected to LC-MS, and the calibration curves for each metabolite were plotted.

4.6. LC Fraction Collection

To get the overview of the general metabolomic differences between the four lens groups, the data on metabolite concentrations in lenses were subjected to a principal component analysis (PCA). The following groups were analyzed: lenses from *S. lucioperca* caught in autumn and in winter, and lenses from *R. rutilus lacustris* caught in autumn and in winter. Figure 3 (left panel) shows the PCA scores plot for the 1st principal component (PC1 = 45.1% of explained variance) versus 2nd component (PC2 = 25.8% of explained variance). The corresponding loadings plot is presented in Figure 3 (right panel).

4.7. Data Analysis

MS/MS spectra of unknown compounds were analyzed with the MetFrag web tool [52] using ChemSpider and PubChem databases. The tool was used for the retrieving compounds from databases according to the measured exact mass and sorting compounds according to the score for the most possible candidates based on exact mass of fragments in MS/MS spectra.

To explore the data and to display the general metabolomic dependences in the data, the principal component analysis (PCA) was performed on a MetaboAnalyst 4.0 web-platform (www.metaboanalyst.ca [32]). PCA scores and loadings plots were constructed with the range data scaling to normalize the contributions of all metabolites.

To reveal the biochemical pathways that are mostly affected by the seasonal variations in the fish lens, we performed the metabolite set enrichment analysis (MSEA) on the MetaboAnalyst platform. MSEA was performed for quantitative data without prior normalization. For the analysis, self-defined metabolite sets were used: 27 metabolic cycles were selected from the 99 pathway-associated metabolite

sets from the Small Molecules Pathways Database (www.smpdb.ca) containing at least one of the quantified metabolite. The rest of the pathways were excluded from the MSEA, as they contained ubiquitous non-informative metabolites (e.g., ATP, ADP, NAD) or did not contain any of the quantified metabolites. The histidine metabolic pathway was extended by the addition of NAH, ovothiol A (OSH), and their precursors described earlier in literature [53,54].

To reveal the statistically-important differences between the groups (lens/gill, seasons), the Mann–Whitney *U*-test was performed using *scipy* (v1.1.0) module on *Python*. The correction of *p*-values for the multiple comparisons by the false discovery rate (FDR) method was done according to the Benjamini–Hochberg procedure using *statsmodels* (v0.9.0) module for *Python*.

5. Conclusions

At the moment, the detailed quantitative metabolomic composition is known for very limited number of tissues and species (except human tissues). One of the few examples of quantitative metabolomic analysis of marine animals is a recent paper by Cappello et al. [28] devoted to the analysis of mussel tissues. In the present work, the concentrations of a broad spectrum of metabolites (68 compounds) in the fish lens and gills are measured for the first time. The obtained quantitative data can be used as baseline levels of metabolites for studying the influence of environmental factors (such as water temperature, DO level, water pollution, diet) on fish health. It is found that the metabolomic composition of the fish lens undergoes strong seasonal variations caused by changes in the DO level, fish feeding activity, and probably other factors. In metabolically passive lens fiber cells, the intracellular defense mostly relies on metabolites—osmolytes and antioxidants. The major lens antioxidant is OSH, while the osmotic protection is provided by the combination of *myo*-inositol, Thr-PETA, Ser-PETA, NAH, and NAA. The concentrations of these compounds and their roles in cytoprotection vary with season: In particular, in the late autumn, NAH and Thr-PETA are the main lens osmolytes, while in February, Ser-PETA and *myo*-inositol become the most abundant osmolytes. In the fish gills, three antioxidants—OSH, GSH, and ascorbate—are present in similar concentrations, and the main osmolytes are *myo*-inositol, taurine, and Ser-PETA. It is important to notice that the main lenticular antioxidant OSH and one of the major lenticular osmolytes NAH are synthesized from the same precursor, amino acid histidine. That indicates the importance of the histidine supply in the fish diet for maintaining homeostasis in the fish lens. The present study was performed for freshwater fish. It would be interesting to compare the metabolomic compositions of tissues of freshwater and marine fish; this work is currently in progress in our laboratory.

Data Availability: The data obtained in this study including NMR raw data, metabolite concentrations, and experimental protocols have been deposited in MetaboLights repository, study identifier MTBLS1057 (https://www.ebi.ac.uk/metabolights/MTBLS1057).

Supplementary Materials: The following are available online at http://www.mdpi.com/2218-1989/9/11/264/s1, Table S1: Characterization of fish lenses and gills used in this study, Table S2: Concentrations of metabolites in nmoles per gram of wet tissue in *Sander lucioperca* and *Rutilus rutilus lacustris*, Table S3: Differences in metabolite content between lenses and gills or seasons, Table S4: Result of Metabolite Sets Enrichment Analysis, Figure S1: NMR spectrum of serine phosphoethanolamine (Ser-PETA), Figure S2: NMR spectrum of threonine phosphoethanolamine (Thr-PETA), Figure S3: ESI-Q-TOF mass-spectrum of CID fragments (MS/MS) of isolated parent ion with m/z 229.0586 (Ser-PETA), Figure S4: ESI-Q-TOF mass-spectrum of CID fragments (MS/MS) of isolated parent ion with m/z 243.0737 (Thr-PETA).

Author Contributions: Conceptualization, Y.P.T. and R.Z.S.; methodology, V.V.Y., E.A.Z. and Y.P.T.; formal analysis, V.V.Y. and A.D.M.; investigation, V.V.Y., E.A.Z. and L.V.Y.; data curation, A.D.M. and Y.P.T.; writing—original draft preparation, Y.P.T. and V.V.Y.; writing—review and editing, Y.P.T., V.V.Y., E.A.Z. and L.V.Y.; supervision—Y.P.T. and R.Z.S.

Funding: This research was funded by Russian Foundation for Basic Research, grant numbers 18-29-13023 in LC-MS measurements, 19-04-00092 in NMR measurements, and 19-34-80008 in sample preparation.

Acknowledgments: We thank Ministry of Science and Higher Education of the RF for the access to NMR and MS equipment.

Conflicts of Interest: The authors declare no conflict of interest.

References

1. Dunn, W.B.; Broadhurst, D.I.; Atherton, H.J.; Goodacre, R.; Griffin, J.L. Systems level studies of mammalian metabolomes: The roles of mass spectrometry and nuclear magnetic resonance spectroscopy. *Chem. Soc. Rev.* **2011**, *40*, 387–426. [CrossRef] [PubMed]
2. Gowda, G.A.; Zhang, S.; Gu, H.; Asiago, V.; Shanaiah, N.; Raftery, D. Metabolomics-based methods for early disease diagnostics. *Expert Rev. Mol. Diagn.* **2008**, *8*, 617–633. [CrossRef] [PubMed]
3. Mishur, R.J.; Rea, S.L. Applications of mass spectrometry to metabolomics and metabonomics: Detection of biomarkers of aging and of age-related diseases. *Mass Spectrom. Rev.* **2012**, *31*, 70–95. [CrossRef] [PubMed]
4. Zhang, A.; Sun, H.; Yan, G.; Wang, P.; Wang, X. Mass spectrometry-based metabolomics: Applications to biomarker and metabolic pathway research. *Biomed. Chromatogr.* **2016**, *30*, 7–12. [CrossRef]
5. Viant, M.R.; Pincetich, C.A.; Tjeerdema, R.S. Metabolic effects of dinoseb, diazinon and esfenvalerate in eyed eggs and alevins of Chinook salmon (Oncorhynchus tshawytscha) determined by 1H NMR metabolomics. *Aquat. Toxicol.* **2006**, *77*, 359–371. [CrossRef]
6. Li, M.-H.; Ruan, L.-Y.; Zhou, J.-W.; Fu, Y.-H.; Jiang, L.; Zhao, H.; Wang, J.-S. Metabolic profiling of goldfish (Carassius auratis) after long-term glyphosate-based herbicide exposure. *Aquat. Toxicol.* **2017**, *188*, 159–169. [CrossRef]
7. Cappello, T.; Maisano, M.; Mauceri, A.; Fasulo, S. 1H NMR-based metabolomics investigation on the effects of petrochemical contamination in posterior adductor muscles of caged mussel Mytilus galloprovincialis. *Ecotoxicol. Environ. Saf.* **2017**, *142*, 417–422. [CrossRef]
8. Cappello, T.; Pereira, P.; Maisano, M.; Mauceri, A.; Pacheco, M.; Fasulo, S. Advances in understanding the mechanisms of mercury toxicity in wild golden grey mullet (Liza aurata) by 1H NMR-based metabolomics. *Environ. Pollut.* **2016**, *219*, 139–148. [CrossRef]
9. Allen, P.J.; Wise, D.; Greenway, T.; Khoo, L.; Griffin, M.J.; Jablonsky, M. Using 1-D 1H and 2-D 1H J-resolved NMR metabolomics to understand the effects of anemia in channel catfish (Ictalurus punctatus). *Metabolomics* **2015**, *11*, 1131–1143. [CrossRef]
10. Remø, S.C.; Hevrøy, E.M.; Breck, O.; Olsvik, P.A.; Waagbø, R. Lens metabolomic profiling as a tool to understand cataractogenesis in Atlantic salmon and rainbow trout reared at optimum and high temperature. *PLoS ONE* **2017**, *12*, e0175491. [CrossRef] [PubMed]
11. Sambraus, F.; Fjelldal, P.G.; Remø, S.C.; Hevrøy, E.M.; Nilsen, T.O.; Thorsen, A.; Hansen, T.J.; Waagbø, R. Water temperature and dietary histidine affect cataract formation in Atlantic salmon (*Salmo salar* L.) diploid and triploid yearling smolt. *J. Fish Dis.* **2017**, *40*, 1195–1212. [CrossRef] [PubMed]
12. Low, C.-F.; Rozaini, M.Z.H.; Musa, N.; Baharum, S.N. Current knowledge of metabolomic approach in infectious fish disease studies. *J. Fish Dis.* **2017**, *40*, 1267–1277. [CrossRef] [PubMed]
13. Bjerkas, E. The role of nutrition in cataract formation in farmed fish. *CAB Rev.* **2006**, *1*, 16. [CrossRef]
14. Jonassen, T.; Hamadi, M.; Remø, S.C.; Waagbø, R. An epidemiological study of cataracts in wild and farmed lumpfish (*Cyclopterus lumpus* L.) and the relation to nutrition. *J. Fish Dis.* **2017**, *40*, 1903–1914. [CrossRef] [PubMed]
15. Wall, A.E. Cataracts in farmed Atlantic salmon (*Salmo salar*) in Ireland, Norway and Scotland from 1995 to 1997. *Vet. Rec.* **1998**, *142*, 626–631. [CrossRef] [PubMed]
16. Breck, O.; Bjerkås, E.; Sanderson, J.; Waagbø, R.; Campbell, P. Dietary histidine affects lens protein turnover and synthesis of N-acetylhistidine in Atlantic salmon (*Salmo salar* L.) undergoing parr–smolt transformation. *Aquac. Nutr.* **2005**, *11*, 321–332. [CrossRef]
17. Remø, S.C.; Hevrøy, E.M.; Olsvik, P.A.; Fontanillas, R.; Breck, O.; Waagbø, R. Dietary histidine requirement to reduce the risk and severity of cataracts is higher than the requirement for growth in Atlantic salmon smolts, independently of the dietary lipid source. *Br. J. Nutr.* **2014**, *111*, 1759–1772. [CrossRef]
18. Waagbø, R.; Trösse, C.; Koppe, W.; Fontanillas, R.; Breck, O. Dietary histidine supplementation prevents cataract development in adult Atlantic salmon, *Salmo salar* L., in seawater. *Br. J. Nutr.* **2010**, *104*, 1460–1470. [CrossRef]
19. Baslow, M.H. Function of the N-acetyl-L-histidine system in the vertebrate eye. Evidence in support of a role as a molecular water pump. *J. Mol. Neurosci.* **1998**, *10*, 193–208. [CrossRef]

20. Rhodes, J.D.; Breck, O.; Waagbo, R.; Bjerkas, E.; Sanderson, J. N-acetylhistidine, a novel osmolyte in the lens of Atlantic salmon (*Salmo salar* L.). *Am. J. Physiol. Regul. Integr. Comp. Physiol.* **2010**, *299*, R1075–R1081. [CrossRef]
21. Bassnett, S. Lens organelle degradation. *Exp. Eye Res.* **2002**, *74*, 1–6. [CrossRef] [PubMed]
22. Snytnikova, O.A.; Khlichkina, A.A.; Yanshole, L.V.; Yanshole, V.V.; Iskakov, I.A.; Egorova, E.V.; Stepakov, D.A.; Novoselov, V.P.; Tsentalovich, Y.P. Metabolomics of the human aqueous humor. *Metabolomics* **2017**, *13*, 5. [CrossRef]
23. Snytnikova, O.A.; Yanshole, L.V.; Iskakov, I.A.; Yanshole, V.V.; Chernykh, V.V.; Stepakov, D.A.; Novoselov, V.P.; Tsentalovich, Y.P. Quantitative metabolomic analysis of the human cornea and aqueous humor. *Metabolomics* **2017**, *13*, 152. [CrossRef]
24. Tsentalovich, Y.P.; Verkhovod, T.D.; Yanshole, V.V.; Kiryutin, A.S.; Yanshole, L.V.; Fursova, A.Z.; Stepakov, D.A.; Novoselov, V.P.; Sagdeev, R.Z. Metabolomic composition of normal aged and cataractous human lenses. *Exp. Eye Res.* **2015**, *134*, 15–23. [CrossRef]
25. Yanshole, V.V.; Snytnikova, O.A.; Kiryutin, A.S.; Yanshole, L.V.; Sagdeev, R.Z.; Tsentalovich, Y.P. Metabolomics of the rat lens: A combined LC-MS and NMR study. *Exp. Eye Res.* **2014**, *125*, 71–78. [CrossRef]
26. Yanshole, V.V.; Yanshole, L.V.; Zelentsova, E.A.; Tsentalovich, Y.P. Ovothiol A is the Main Antioxidant in Fish Lens. *Metabolites* **2019**, *9*, 95. [CrossRef]
27. Zelentsova, E.A.; Yanshole, L.V.; Snytnikova, O.A.; Yanshole, V.V.; Tsentalovich, Y.P.; Sagdeev, R.Z. Post-mortem changes in the metabolomic compositions of rabbit blood, aqueous and vitreous humors. *Metabolomics* **2016**, *12*, 172. [CrossRef]
28. Cappello, T.; Giannetto, A.; Parrino, V.; Maisano, M.; Oliva, S.; De Marco, G.; Guerriero, G.; Mauceri, A.; Fasulo, S. Baseline levels of metabolites in different tissues of mussel Mytilus galloprovincialis (Bivalvia: Mytilidae). *Comp. Biochem. Physiol. Part D Genom. Proteom.* **2018**, *26*, 32–39. [CrossRef]
29. Gowda, G.A.; Raftery, D. Quantitating metabolites in protein precipitated serum using NMR spectroscopy. *Anal. Chem.* **2014**, *86*, 5433–5440. [CrossRef]
30. Yanshole, V.V.; Yanshole, L.V.; Snytnikova, O.A.; Tsentalovich, Y.P. Quantitative metabolomic analysis of changes in the lens and aqueous humor under development of age-related nuclear cataract. *Metabolomics* **2019**, *15*, 29. [CrossRef]
31. Terzhevik, A.; Golosov, S. Dissolved Oxygen in Ice-Covered Lakes. In *Encyclopedia of Lakes and Reservoirs*; Bengtsson, L., Herschy, R.W., Fairbridge, R.W., Eds.; Springer Netherlands: Dordrecht, The Netherlands, 2012; pp. 220–222.
32. Chong, J.; Soufan, O.; Li, C.; Caraus, I.; Li, S.; Bourque, G.; Wishart, D.S.; Xia, J. MetaboAnalyst 4.0: Towards more transparent and integrative metabolomics analysis. *Nucleic Acids Res.* **2018**, *46*, W486–W494. [CrossRef] [PubMed]
33. Mathias, R.T.; Kistler, J.; Donaldson, P. The lens circulation. *J. Membr. Biol.* **2007**, *216*, 1–16. [CrossRef] [PubMed]
34. Mathias, R.T.; Rae, J.L. Transport properties of the lens. *Am. J. Physiol.* **1985**, *249*, C181–C190. [CrossRef] [PubMed]
35. Mathias, R.T.; Rae, J.L. The lens: Local transport and global transparency. *Exp. Eye Res.* **2004**, *78*, 689–698. [CrossRef]
36. McNulty, R.; Wang, H.; Mathias, R.T.; Ortwerth, B.J.; Truscott, R.J.W.; Bassnett, S. Regulation of tissue oxygen levels in the mammalian lens. *J. Physiol.* **2004**, *559*, 883–898. [CrossRef] [PubMed]
37. Hand, C.E.; Honek, J.F. Biological chemistry of naturally occurring thiols of microbial and marine origin. *J. Nat. Prod.* **2005**, *68*, 293–308. [CrossRef]
38. Varma, S.D. Ascorbic Acid and the Eye with Special Reference to the Lens. *Ann. N. Y. Acad. Sci.* **1987**, *498*, 280–306. [CrossRef]
39. Wu, G.; Fang, Y.-Z.; Yang, S.; Lupton, J.R.; Turner, N.D. Glutathione metabolism and its implications for health. *J. Nutr.* **2004**, *134*, 489–492. [CrossRef]
40. Holler, T.P.; Hopkins, P.B. Ovothiols as biological antioxidants. The thiol groups of ovothiol and glutathione are chemically distinct. *J. Am. Chem. Soc.* **1988**, *110*, 4837–4838. [CrossRef]
41. Mirzahosseini, A.; Noszál, B. Species-specific thiol-disulfide equilibrium constants of ovothiol A and penicillamine with glutathione. *RSC Adv.* **2016**, *6*, 26757–26764. [CrossRef]

42. Mirzahosseini, A.; Orgován, G.; Hosztafi, S.; Noszál, B. The complete microspeciation of ovothiol A, the smallest octafarious antioxidant biomolecule. *Anal. Bioanal. Chem.* **2014**, *406*, 2377–2387. [CrossRef] [PubMed]
43. Weaver, K.H.; Rabenstein, D.L. Thiol/Disulfide Exchange Reactions of Ovothiol A with Glutathione. *J. Org. Chem.* **1995**, *60*, 1904–1907. [CrossRef]
44. Marjanovic, B.; Simic, M.G.; Jovanovic, S.V. Heterocyclic thiols as antioxidants: Why ovothiol C is a better antioxidant than ergothioneine. *Free Radic. Biol. Med.* **1995**, *18*, 679–685. [CrossRef]
45. Ariyanayagam, M.R.; Fairlamb, A.H. Ovothiol and trypanothione as antioxidants in trypanosomatids. *Mol. Biochem. Parasitol.* **2001**, *115*, 189–198. [CrossRef]
46. Palumbo, A.; d'Ischia, M.; Misuraca, G.; Prota, G. Isolation and structure of a new sulphur-containing aminoacid from sea urchin eggs. *Tetrahedron Lett.* **1982**, *23*, 3207–3208. [CrossRef]
47. Palumbo, A.; Misuraca, G.; d'Ischia, M.; Donaudy, F.; Prota, G. Isolation and distribution of 1-methyl-5-thiol-l-histidine disulphide and a related metabolite in eggs from echinoderms. *Comp. Biochem. Physiol. B* **1984**, *78*, 81–83. [CrossRef]
48. Turner, E.; Klevit, R.; Hager, L.J.; Shapiro, B.M. Ovothiols, a family of redox-active mercaptohistidine compounds from marine invertebrate eggs. *Biochemistry* **1987**, *26*, 4028–4036. [CrossRef]
49. Turner, E.; Klevit, R.; Hopkins, P.B.; Shapiro, B.M. Ovothiol: A novel thiohistidine compound from sea urchin eggs that confers NAD(P)H-O2 oxidoreductase activity on ovoperoxidase. *J. Biol. Chem.* **1986**, *261*, 13056–13063.
50. Castellano, I.; Di Tomo, P.; Di Pietro, N.; Mandatori, D.; Pipino, C.; Formoso, G.; Napolitano, A.; Palumbo, A.; Pandolfi, A. Anti-Inflammatory Activity of Marine Ovothiol A in an In Vitro Model of Endothelial Dysfunction Induced by Hyperglycemia. *Oxid. Med. Cell Longev.* **2018**, *2018*, 2087373. [CrossRef]
51. Tamara, S.O.; Yanshole, L.V.; Yanshole, V.V.; Fursova, A.Z.; Stepakov, D.A.; Novoselov, V.P.; Tsentalovich, Y.P. Spatial distribution of metabolites in the human lens. *Exp. Eye Res.* **2016**, *143*, 68–74. [CrossRef]
52. Ruttkies, C.; Schymanski, E.L.; Wolf, S.; Hollender, J.; Neumann, S. MetFrag relaunched: Incorporating strategies beyond in silico fragmentation. *J. Cheminform.* **2016**, *8*, 3. [CrossRef] [PubMed]
53. Baslow, M.H.; Guilfoyle, D.N. N-acetyl-l-histidine, a Prominent Biomolecule in Brain and Eye of Poikilothermic Vertebrates. *Biomolecules* **2015**, *5*, 635–646. [CrossRef] [PubMed]
54. Naowarojna, N.; Huang, P.; Cai, Y.; Song, H.; Wu, L.; Cheng, R.; Li, Y.; Wang, S.; Lyu, H.; Zhang, L.; et al. In Vitro Reconstitution of the Remaining Steps in Ovothiol A Biosynthesis: C-S Lyase and Methyltransferase Reactions. *Org. Lett.* **2018**, *20*, 5427–5430. [CrossRef] [PubMed]